Expert Views

Parametric Insurance: A 360° View

Part Three of Three

SCOR
The Art & Science of Risk

April 2024

Parametric Outside the Box

This third issue of our parametric series challenges plain vanilla natural catastrophe covers. Part of SCOR's value proposition is the full alignment of every solution with the needs of the cedant concerned. This requires a mutual understanding of the risk situation and the risk transfer solution. Without this, there is a strong possibility that a simpler or cheaper – but inadequate – cover will be chosen.

An adequate cover needs to optimize the basis risk and be accepted by the (re)insurance market. Non-acceptance could result in uncovered capacity and additional efforts during the first renewals.

Uncontrolled basis risk can put the cedant, rather than the carrier, in financial difficulty if no recovery is paid in the event of an ultimate financial loss. We will try to address the latter situation in the subsequent paragraphs.

In our Parametric Mishaps section, we illustrate how cyclones and earthquakes can sometimes evade measurement and miss triggering a loss, before looking at designs that can improve this situation.
We then look at Event Map Design as a way of reducing basis risk. Event Map Design works for both single locations and distributed portfolios. In our view, it should become the standard for natural catastrophes now that the required data is available worldwide. We explain how the underlying risks can be modelled and how the basis risk can be analyzed.

Parametric Mishaps

Measuring at the Source or at the Location

In 1992, Hurricane Andrew roared along the coast of the Gulf of Mexico, from Florida to Louisiana. As an extreme hurricane, it left severe structural damage in its wake. From a reanalysis conducted by engineers ten years later, wind gusts must have exceeded 165 miles per hour (265 kilometers per hour)[1]. It showed that sustained wind measurements were underestimated by around 20 mph (32 kph). Anemometers in the most affected spots failed to measure anything at all. A quarter of a century later, measurements proved unreliable for Irma too. Even before the peak of the storm, 22 out of 102 wind stations failed[2].
We understand that hurricane observations rely on a multitude of measurement sources, which overall are robust. Our purpose in looking at failing measurements here is to trigger a discussion on the reliability of measuring an event at its source for a parametric cover.

In 2007, Cyclone Gamède chose a path that went around the island of La Réunion. Given its distance of more than 200 km from the island, one could have been forgiven for expecting little damage to occur. Mother Nature, however, is inventive. The cyclone remained static for five long days offshore, and nearly five meters of rain poured down within 96 hours, leading to diluvian meteorological conditions. Waves up to 12 meters high eroded beaches and damaged coastal infrastructure.

Figure 1: Cyclone Gamède remained static alongside La Réunion

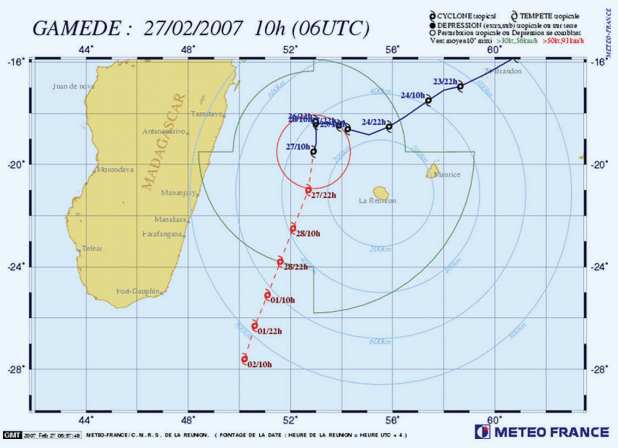

Source: Meteo France C.N.R.S de la Réunion, 2007[3]

Much can happen between the eye of a hurricane and the location of the exposure. Measurements at the location provide estimates of the intensity of a hazard and of its impact on insured assets. Typhoon Hato struck Hong Kong in August 2017, with a maximum wind speed recorded in the vicinity of Hong Kong of 139 km per hour. It caused massive damage to the country, generating an economic loss of approximately HKD 1.2 billion. Hato is one of the strongest typhoons to impact Hong Kong over the past 50 years, a scale which necessarily requires insurance support.

Let's turn back time now to 2008. Typhoon Fengshen had just passed across the island, and the memory of Typhoon Dujuan in 2003 was still fresh in people's minds.

The economic losses for Fengshen and Dujuan were small, but the frequency of such events was starting to worry us. We remembered a visit by a cat-in-a-box expert and requested his advice on a parametric cover. He suggested a 60-kilometer radius for payout. Less than a decade later, the first mishap struck us, as Hato was just outside the 60-kilometer radius and the cover simply did not trigger past this point.

Typhoon Hato battered Hong Kong despite passing by far offshore

Source: Hong Kong Observatory, 2019

Figure 2: A 60-kilometer radius around Hong Kong would have excluded payouts for Typhoon Hato. An 80-kilometer radius would have excluded payouts for Typhoon Mangkhut

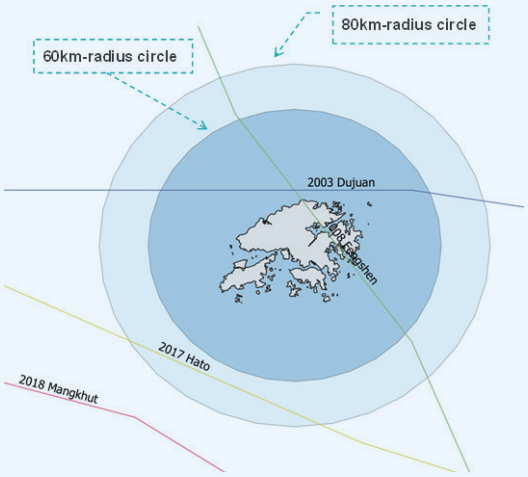

Source: SCOR APAC Cat Risk Modelling team

Obviously, we were in dire need of an effective cover, so the expert suggested extending the radius to 80 km. Just one year later, Typhoon Mangkhut proved him wrong again, causing a massive economic loss to the tune of HKD 4.6 billion. Experts may argue that step payouts could have been introduced, that the cover was not well calibrated, and so on. And of course, that a larger perimeter could have been foreseen. Nonetheless, the cat-in-a-box design has the significant shortcoming of potentially missing severe events, leading to a mismatch between actual damage and parametric payout.

In June 2019, the press reported a USD 60 million partial payout from the CAR 120 cat bond covering Peru[6]. The event was a magnitude-8 earthquake deep in the Amazon. The earthquake was strong, but it was also 123km deep, and the intensity displayed on the map in figure 3 faded quickly towards inhabited regions. This led to minor damage and an economic loss of USD 50 million. The cat-in-a-box design triggered a partial settlement of 30% of USD 200 million.

Figure 3: Missed Trigger for Earthquake. In 2019, a very severe earthquake shook the Lagunas District in the Peruvian Amazon

Marcroseismic Intensity Map
USGS ShakeMap: 78 km SE of Lagunas, Loreto, PE
May 26, 2019 07:41:15 UTC M8.0 S5.81 W75.27 Depth: 122.6km ID:us60003sc0

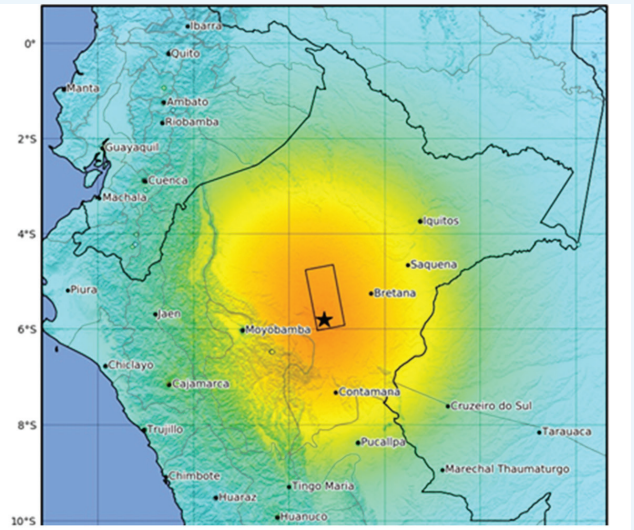

SHAKING	Not felt	Weak	Light	Moderate	Strong	Very strong	Severe	Violent	Extreme
DAMAGE	None	None	None	Very light	Light	Moderate	Moderate/heavy	Heavy	Very heavy
PGA(%g)	<0.05	0.3	2.76	6.2	11.5	21.5	40.1	74.7	>139
PGV(cm/s)	<0.02	0.13	1.41	4.65	9.64	20	41.4	85.8	>178
INTENSITY	I	II-III	IV	V	VI	VII	VIII	IX	X+

Scale based on Worden et al. (2012) Version 7: Processed 2019-08-03T04:50:40Z
△ Seismic Instrument ○ Reported Intensity ★ Epicenter ▭ Rupture

Source: US Geological Survey[5], search from ShakeMap Archives

As positioned on the map above, the Pisco event of August 15, 2007, which had a magnitude of 8.0 and an epicenter close to habitation, would have triggered a full payout from its USD 200 million cover. Nevertheless, much higher economic losses of USD 600 million were reported[7]. Further back in time, on June 23, 2001, the magnitude-8.4 event close to Arequipa would not have paid out at all. But the economic losses involved amounted to USD 300 million, which is commensurate with the high Mercali Intensities of 6.5 to 7 reported in the neighboring cities.

Figure 4: Three historical earthquakes in Peru (2001 in Arequipa, 2007 in Pisco, 2019 in Lagunas) illustrate how payout, based on location and magnitude only, partially captures the ultimate financial impact

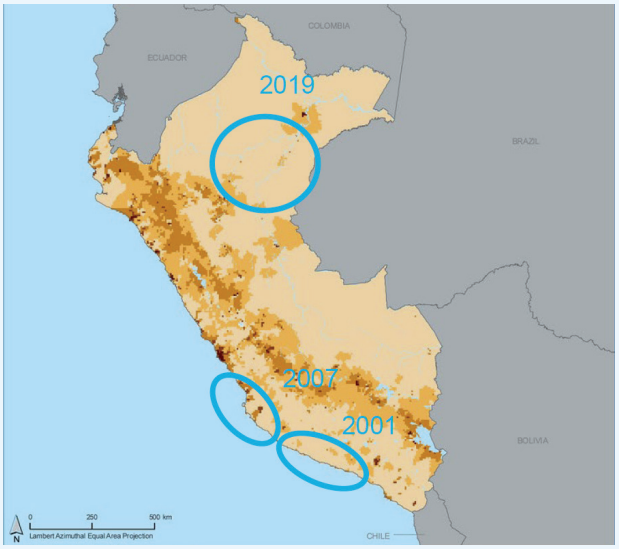

Source: US Geological Survey, 2023[5]

Back testing on payment performance unveils earthquake characteristics that should not be neglected in a parametric design. The location of the epicenter within a box needs to be relativized. A magnitude-8 event means a 200-kilometer-long fault rupture. This is more than a typical cat-in-box boundary of 100 kilometers. Depth and soil condition determine how (and if) shockwaves are propagated to inhabited surfaces. Local ground shaking intensity matters where the population is concentrated, rather than at the position of the epicenter.

Improving Earthquake Covers

Figure 5: ShakeMap from the 2004 earthquake in Al Hoceima, Morocco

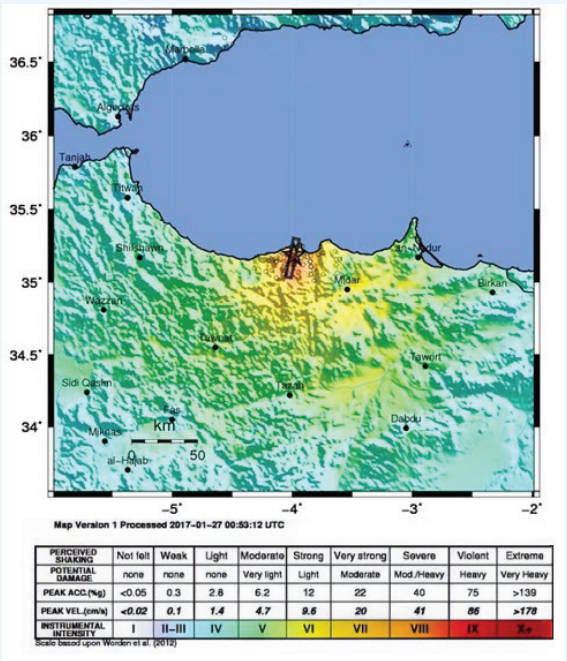

Source: US Geological Survey, 2023[5]

In 2004, the inhabitants of Al Hoceima, Morocco, were woken up during the night by a violent earthquake. The 6.3-magnitude quake shook the city to its core: the epicenter was right beneath it. The death toll reached 631, with 926 people injured and the livelihoods of more than 2,500 people impacted. The market suffered a loss of MAD 707 million, or EUR 67 million at today's conversion rate. Intensities of up to 9 were measured on the Modified Mercalli Intensity scale. Just 13 kilometers to the west of Al Hoceima, a 1994 earthquake with a similar magnitude of 6.0 had caused three deaths and a market loss of EUR 1 million. Why was there such a relatively low impact? The sub-soil conditions meant that shaking from seismic waves attenuated quickly, and low intensities were measured at the core of the city. Similarly, in 2016, a 6.3-magnitude earthquake occurred off the shore of Al Hoceima with literally no impact.

Figure 6: Epicenters from three historical earthquakes in the vicinity of Al Hoceima, Morocco, overlayed on a map of population density

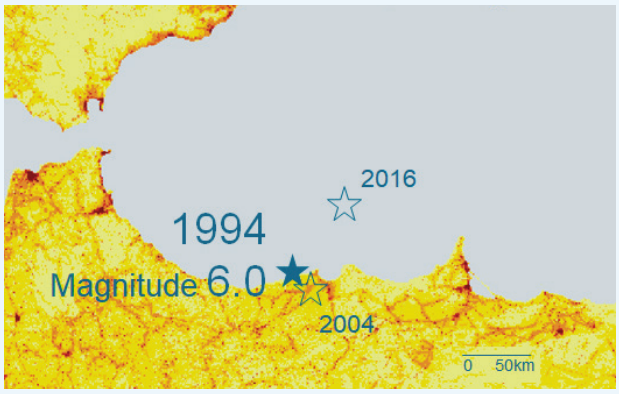

Source: population density map created by SCOR based on data[8]

What would a cat-in-a-circle solution have looked like, with a radius around the city of some 20 kilometers or more? With similar magnitudes, these events could all have paid out a similar amount.

We suggest using so-called shakemaps instead (as seen on the next page). Shakemaps are produced by geological institutes in quasi-real time. From the first seismic records, an intensity is calculated on a fine grid (1x1 km) using physical models. It is further refined using successively finite fault models[5], the strong motion network, and, finally, so-called DYFI (Did You Feel It?) confirmation by the impacted population. Within two weeks, precise and public information is available, which we use to constitute our parametric index.

Figure 7: Evolution of ShakeMap over two weeks, here for the Mw-6.0 earthquake of September 26, 1997, in Umbria-Marche, Italy

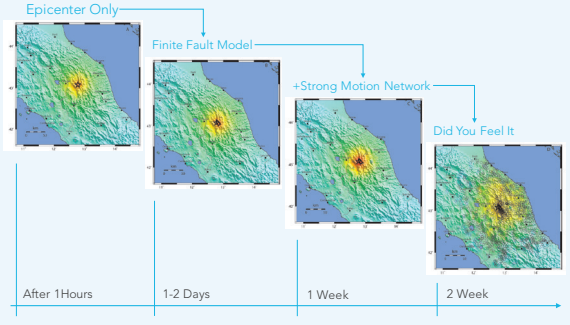

Source: Allend, 2008[9]

Improving Tropical Cyclone Covers

Keeping the Hato and Mangkhut mishaps in mind, we turn to the public resources from the World Meteorological Organization (WMO). Embedded within the United Nations, WMO stretches across 193 countries to provide data exchange, information and research with member meteorological institutions. As illustrated in Figure 8, five tropical cyclone bodies operate in their respective regions, publishing regular bulletins with the latest meteorological information.

WMO's Global Observing System captures hazard components such as wind speed, pressure, wind direction and precipitation, based on a number of different observations including aircraft, satellite, marine, surface, upper-air and weather radar observations.

We suggest using these hazard components in conjunction with wind field models. The Willoughby model considers the eyewall coordinates of a cyclone and the maximum windspeed along its track.

Figure 8: Tropical Cyclone Regional Bodies

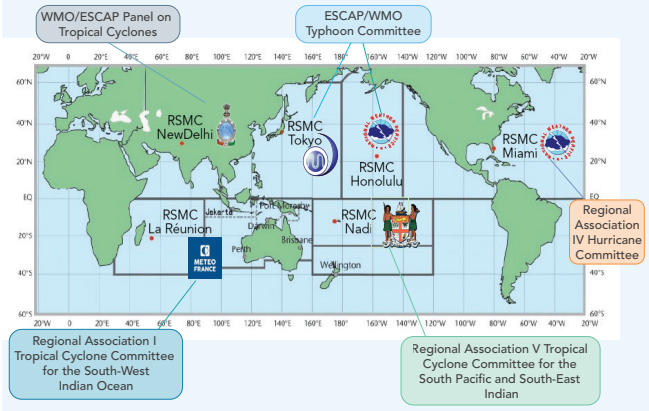

WMO, retrieved from Tropical Cyclone Regional Bodies[10]

Typically, every six hours, reporting agencies like NOAA calculate storm motion parameters such as forward speed, the radius of maximum winds, and the decay rate of winds. Applying the Willoughby model to each parameter produces an intensity map, with estimated windspeeds plotted on a fine grid along both sides of the track.

Figure 9: Global Observing System initiated for the World Weather Watch

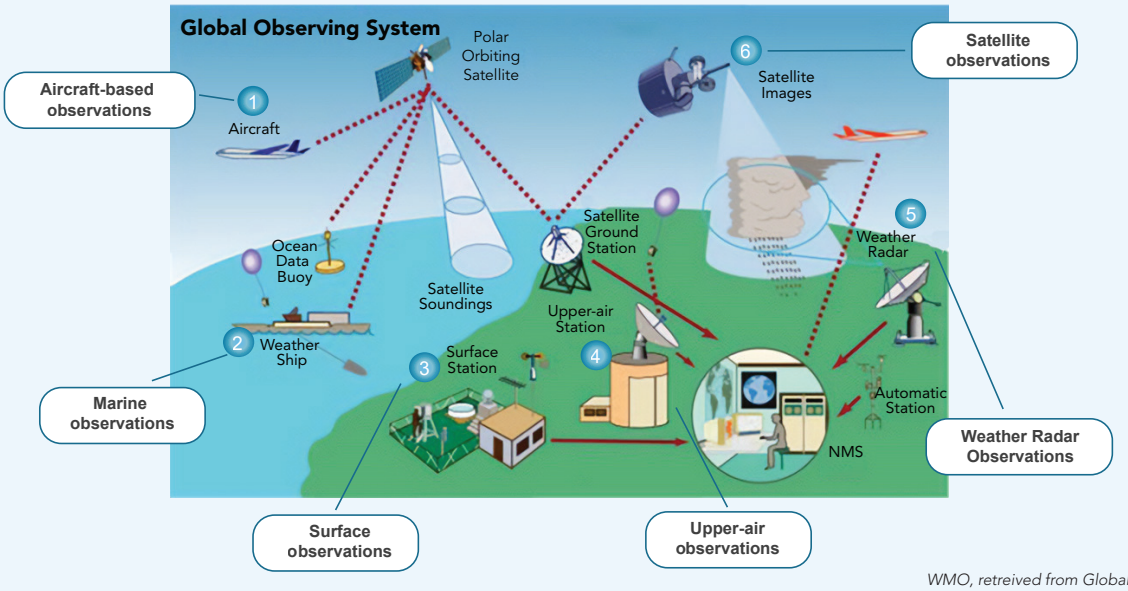

WMO, retreived from Global Observing[11]

Figure 10: Wind profile from a parametric representation by Willoughby et al.

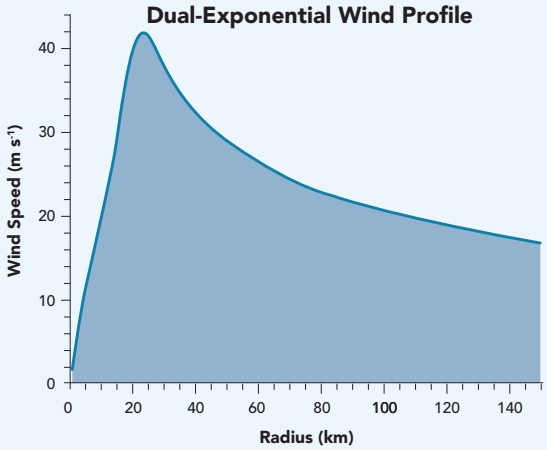

Source: Willoughby, 2006[12]

Our Parametric Mishaps section showcased the benefits of using intensity maps. These bring the intensity measurement of a natural catastrophe to the location of the exposure. The design of such solutions mirrors the four-step approach to hazard modelling, as per Figure 12. The Exposure is required on a grid, or on geolocalized areas which is overlaid by the intensity map. The exposure amount provided at each grid point corresponds to the sum insured at that location. The Vulnerability is a function of the measured intensity at each grid point. By applying the Vulnerability to the Exposure, we can calculate the payout at each grid point. The total payout is obtained by adding everything up over the entire grid. The intensity map allows us to estimate a loss incurred by the underlying risk, be it property damage or a defined compensation scheme. The product is designed to focus on the alignment between loss and payout. The final step is risk transfer, which occurs in the same flexible way as for a traditional cover.

Figure 11: Path and wind speed of Hurricane Dorian moving up the East Coast of the USA

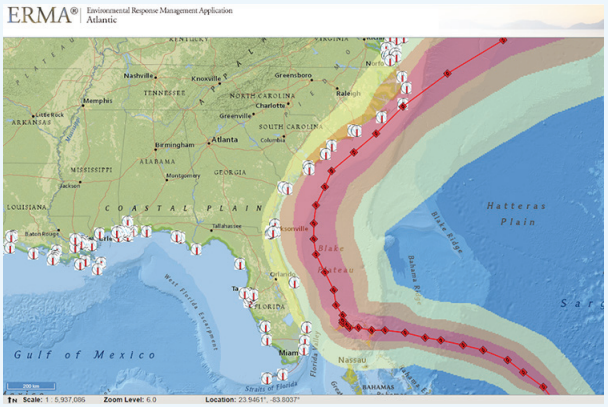

Source: NOAA, 2019[13]

Figure 12: Event map design

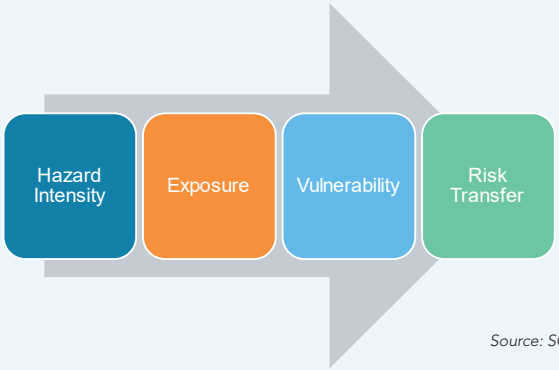

Source: SCOR

Application to Earthquake

Returning to the Moroccan examples we looked at earlier, we can envisage a national residential cover. Morocco suffers from low insurance penetration. This cover should help the uninsured population to receive compensation if their homes become inhabitable. In the absence of data from the insurance industry, exposure and vulnerability need to be defined as part of the parametric design.

Census data provides detailed statistics on population and homes, together with the type and age of the construction. The granularity at commune level is too coarse for this study. We estimated that a shift of 5 km in the exposure concentration impacts the loss estimate by 2%. Population density data is used to disaggregate communal data to a finer grid, with a mesh of 1 km. Such data is reconstructed by the European Commission using satellite images and is freely accessible.

Figure 13: Number of buildings by commune in Morocco

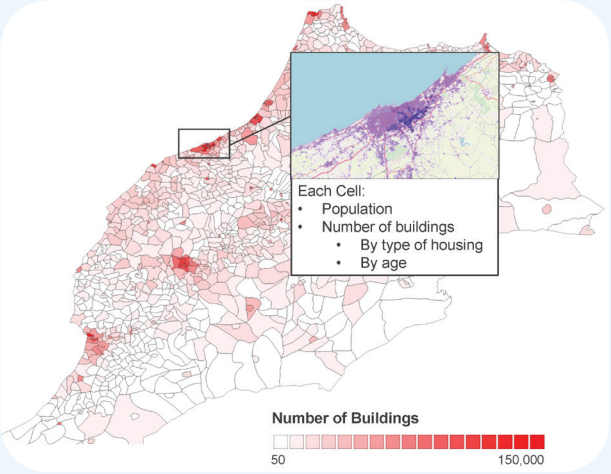

Source: map reconstructed by the EMEA Cat Modelling team based on the 2014 Global Human Settlement, a.d data.[8]

To reflect the criterium of inhabitability, we use the probability of building collapse, published by the National School of Architecture[13] as a payout function (vulnerability). This allows us to distinguish seven exposure classes. A city like Agadir, which was reconstructed after the earthquake of 1960, has followed more resistant standards than old cities like Fès. Careful attention to basis risk justifies aligning the payout calculation with specific vulnerabilities in various areas.

Figure 14: Payout function from probability of building collapse

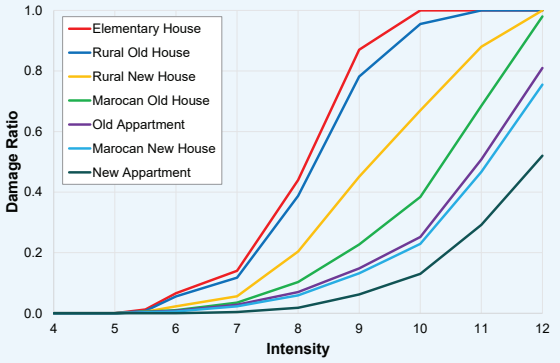

Source: SCOR Alternative Solutions team from Harrouni, 2009[14]

The table below illustrates the index calculation at exemplary grid points for one stochastic event. At each grid point, an intensity is taken from the event shakemap. The exposure of each vulnerability class, respectively, is multiplied by the payout to obtain its individual index. In total, the event leads to a payout of MAD 450 million.

Figure 15: Illustration of index payout outcome in MAD for specific building types at illustrative grid points (Cell), with intensity (MMI) and payout function (vulnerability) applied to the related Exposure

Cell	MMI	Building type	Exposure	Payout	Index
1	8	Elementary House	500'000	42%	210'000
1	8	Appartment Old	880'000	10%	88'000
2	4	Rural House Old	1'265'000	0%	0
2	4	Rural House New	715'00	0%	0
3	9	Elementary House	1'000'000	86%	860'000
3	9	Moroccan House Old	105'000	22%	231'000
3	9	Appartment New	800'000	9%	72'000
-	-	-	-	-	-
Total					**450'000'000**

Source: SCOR Alternative Solutions team[15]

The design is complete when we have proof that adequate payout is recovered. Agadir suffered a 5.9-magnitude earthquake in 1960. Most parts of the city were destroyed. By feeding our calculation with a historical shakemap, we get a property loss estimate of MAD 4.3 billion for this event. Our calculation for the Al Hoceima 1994 event leads to an estimated property loss of around MAD 650 million. This method allows us to consider events that are remote in time and space – for example, shakemaps even exist for events like the Lisbon earthquake of 1755, which also shook northern Morocco by intensity of up to 7 on the MMI scale. The 1960 and 1994 earthquakes in Morocco also produced an intensity of up to 7 on the MMI scale. These two events were disastrous.

In Agadir (1960), 12,000 people died and 75% of the buildings were destroyed. New buildings were reconstructed following improved standards, which is taken into account in this analysis. In Al Hoceima (1994), more than 600 people died and 15,000 were left homeless due to the collapse of 2,500 houses, leading to a strong economic

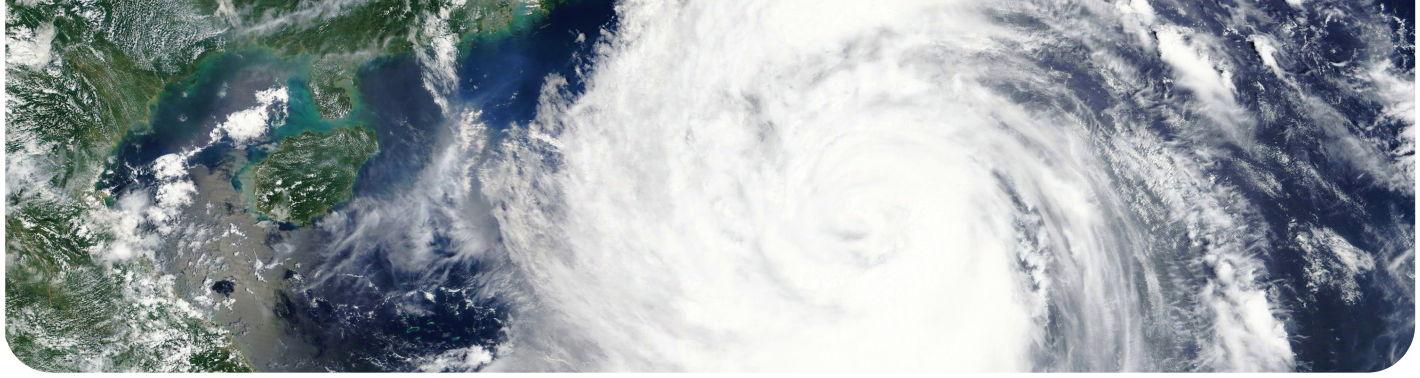

loss[15]. The market index loss calculated using the approach above can be compared to the expected recovery from such historical events. The appetite of the risk cedant to retain part of the market index loss can be reflected in risk transfer schemes that are similar to traditional indemnity reinsurance, as illustrated in Figure 16.

The risk transfer is a matter of risk appetite. The cedant can align the effective recovery with its available capital with just a deductible. The limit will be commensurate with the severity of a fully covered event. The advantage of designing the index loss from the ground up is that you gain transparency in the underlying design, as well as helping to align risk appetite between risk carrier and risk cedant.

Figure 16: Illustration of a cession from the index-based market loss

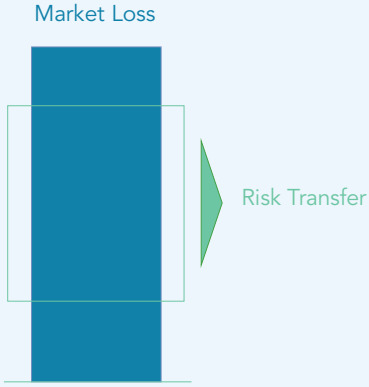

Source: SCOR Alternative Solutions team[15]

Application to Tropical Cyclones

Figure 17: Peak gusts for Typhoon Mangkhut by district, greater Hong Kong area

Source: SCOR APAC Cat Modelling team

Figure 18: Population density as a proxy for asset distribution by district, greater Hong Kong area

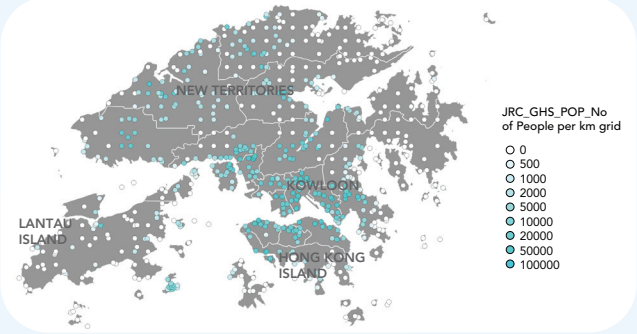

Source: SCOR APAC Cat Modelling team based on (Global Human Settlement, s.d.) data[8]

To illustrate the application of the Willoughby model to tropical cyclones, let's go back to 2018 and Hong Kong's Typhoon Mangkhut, which we looked at earlier in our Missed Trigger for Cyclone section.

In figure 17, the dots become progressively darker as the wind intensity for Typhoon Mangkhut increases. The intensity is calculated using the Willoughby model. You can see that the strongest wind speeds are in the South-Western island of Lantau, closest to the track of the typhoon. For the purposes of this exercise, we assume that the distribution of covered assets is reflected by the population density. The highest density can be seen in Kowloon and Hong Kong islands, as illustrated in the adjacent figure 18.

The damage ratio is calculated from the wind field intensity at each dot, applying the payout or vulnerability functions. The ratio is at its strongest at the tip of Lantau, as shown in Figure 19 on the next page. This is an immediate consequence of the higher wind speeds.

The strongest concentration of population and assets is what drives the indexed loss. You can see this in Figure 20 with the higher values shown for Kowloon and Hong Kong islands. The sum of the indexed loss on all dots provides the total loss.

Figure 19: Damage ratio derived from peak gusts by district, greater Hong-Kong area

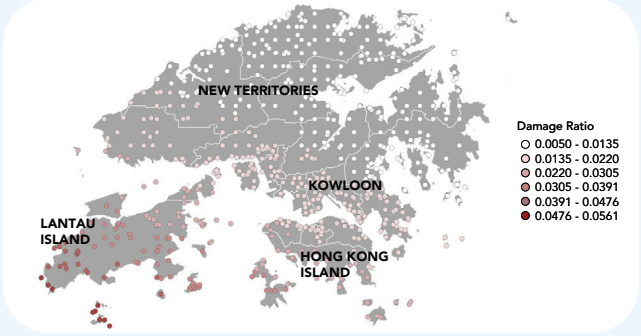

Source: SCOR APAC Cat Modelling team[16]

Figure 20: Index Loss calculated by district, greater Hong-Kong area

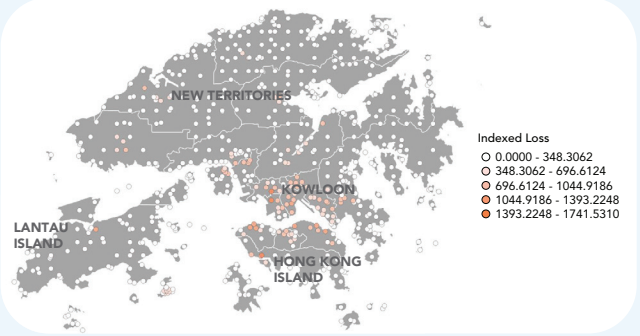

Source: SCOR APAC Cat Modelling team[14]

With the event map approach, we reproduce the market loss, taking into account local effects from hazard intensity, exposure concentration, and vulnerability.

Risk Modelling

Once the needs and requirements of the parametric risk-transfer mechanism are defined, market acceptance will depend on its price. How much will the cover cost the insured? At what price will risk carriers take on part of this risk, and how will it accumulate within their current portfolio? Which parameters in the design are most sensitive to price?

Just like for traditional insurance products, the key element for pricing here is the expected Average Annual Loss (AAL) to which other charges will be added. We use stochastic catalogues from natural catastrophe models containing detailed information for each synthetic event, as shown in Figure 21, including location, intensity, magnitude, hazard footprints, and probability of occurrence. Most of the time, the information is not readily available and (sometimes tedious) work is needed to retrieve this data from the models.

Leveraging this information, we reproduce the indices and the parametric product payout for every single event in the simulated catalogue. This gives us an event loss table, with which we can easily calculate the triggering probability and the AAL.

Simple statistics help decision-making while designing the product. How frequently is the cover likely to be activated on average? What is the average return period of an event with full payout?

Figure 21: RMS stochastic catalogue earthquake events in Morocco at their epicenters, with increasing bubble size for Richter scale magnitude. For illustrative purposes, one event is shown with colored contour lines for its intensity shakemap

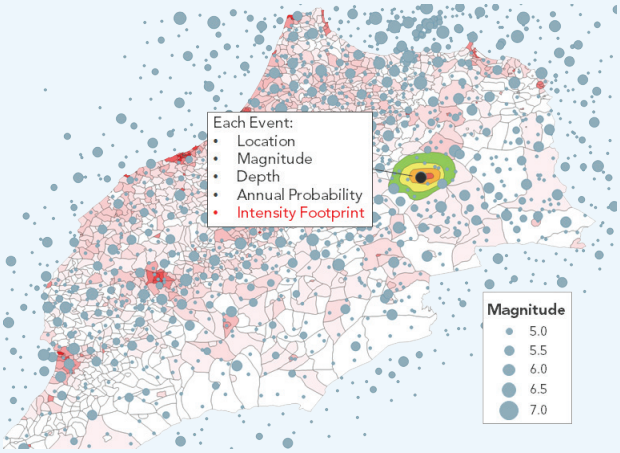

Source: SCOR EMEA Cat Modelling team, using RMS risk modelling catalogue and back-engineered event intensity ShakeMap.

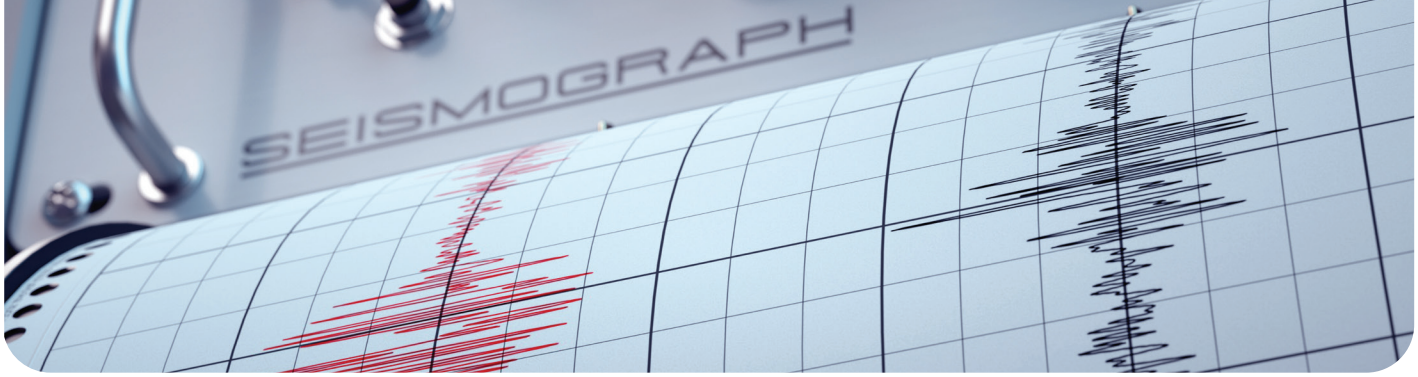

We illustrate this risk analysis approach in the framed earthquake example hereafter[17]:

Modelling Parametric Cat Cover

A simple cat-in-a-region cover is defined by:

Trigger: An earthquake of magnitude (Mw) 6.7 or above with an epicenter on the belt stretching from Istanbul to Izmir, as shown in Figure 22 below.

Payout: EUR 50,000,000

Data Provider: USGS
Based on the stochastic catalogue, triggering events activate the cover 11,000 times. This represents 11% of all events, corresponding to one full loss every nine years. The AAL amounts to EUR 5.5 million.

Figure 22: Events of Mw 6.7 or above with epicenter within the region of the deal in the stochastic catalogue of the catastrophe model representing 100k-year simulation

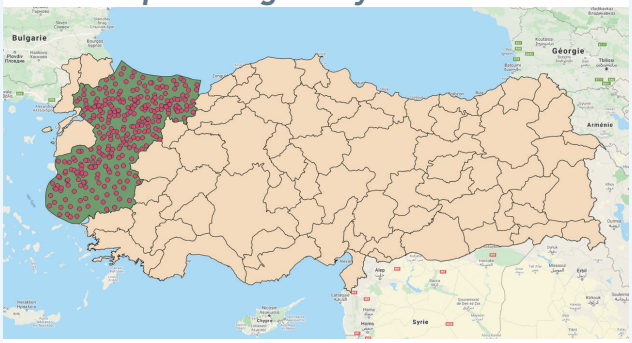

Source: SCOR nat cat modelling resources

Cat modelling tools are essentially calibrated for property damage portfolios. We push them to the limit with parametric products. A deep understanding of the models and their components is fundamental.

It requires expertise to:
- extract data in the right format,
- use modelling modules in isolation, and
- calibrate our own view of the risk.

Challenging our outcome using historical events with a magnitude of more than 6.7, we notice in the last 70 years that five events would have triggered the cover, while many others would have come very close to doing so. Considering the latter with some weighting factors, we come close to seven to nine events, in line with our stochastic outcome.

Figure 23: Historical earthquakes in Eastern Turkey since 1950 with Mw ≥ 6.7

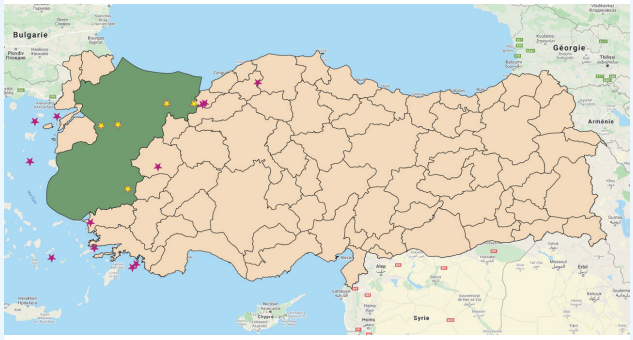

Source: SCOR nat cat modelling resources

It should be noted that an event of Mw 6.7 with an epicenter just outside of the region, or a Mw 6.6-event within the region, would certainly produce damage and significant losses in the provinces of the deal. But it would not trigger any recovery. Step payout functions inherently introduce payout uncertainty, adding to the basis risk.

Basis Risk Analysis

Selecting earthquake events out of the RMS stochastic catalogue with zero payout leads to the blue dots represented in Figure 24. Their location points to their respective epicenters, and their size corresponds to their magnitude. On the mainland, the dots are small for magnitudes below 5, and slightly larger in mountainous inhabited regions. No dot comes close to an area with high population density. Offshore, higher-magnitude events are displayed, up to 6.5. All these dotted events would lead to low or no intensity in inhabited regions, which verifies the first case of basis risk.

Figure 24: RMS stochastic catalogue earthquake events in Morocco that would have led to no payout

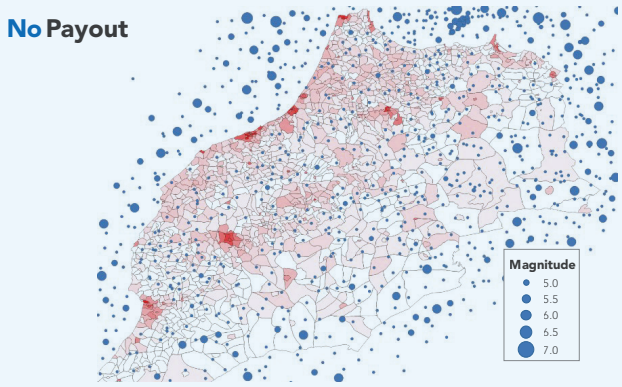

Source: SCOR EMEA Cat Modelling team using RMS risk modelling catalogue

Conversely, full payout events are shown in Figure 25. Larger dots for magnitudes above 6 are distributed across the country in populated regions. In high-density areas, smaller-magnitude dots can also be observed. For both, the local intensity will be high enough at the location of the exposure to trigger a full payout, which verifies the second case of basis risk.

No payout for a damaging event, or a payout while the exposure is untouched, are both extreme cases of basis risk, which we illustrate below.

Figure 25: RMS stochastic catalogue earthquake events in Morocco that would have led to a full payout

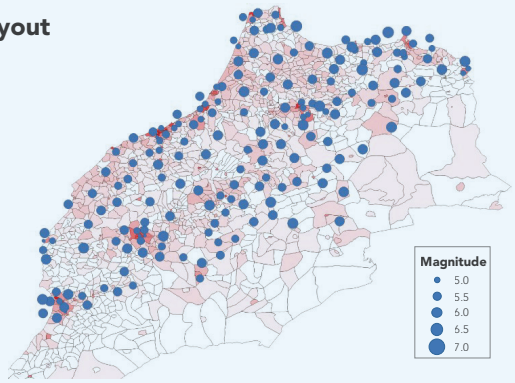

Source: SCOR EMEA Cat Modelling team using RMS risk modelling catalogue

Both examples provide visual proof, independent of the index calculation, that the basis risk is well controlled at the extreme. For the sake of brevity, we omit showing a third plot presenting partial payout, which illustrates how payout is commensurate with moderate events.

We must stress here how important it is for the index design to match the level of detail required for a stochastic model. Any discrepancy due to a coarser design would lead to basis risk at the expense of the protection buyer. As an illustration, our analyses show that a shakemap displacement of at least 5 km leads to an impact on the index loss in the range of 5-15%. Capturing the exact location of exposure and suffered intensity is a key element of such designs. The solution is calibrated by comparing its payout outcome for historical events. We want the calibration to be consistent across different geographies, for different types of buildings and their respective vulnerabilities. This means that any change in the solution's parameters, e.g., the vulnerability function for specific building types, should be reflected across the entire geography as measured by applying the historical or stochastic event intensity maps. It is important for the approach to create no biases that would inflate or deflate payout outcomes for some events, to the detriment of others.

Having looked at parametric insurance both inside and outside the box over this series, it's time to wrap the box up

COP28 in December 2023 showcased growing evidence of risk analytics capabilities within the insurance spectrum. The US National Association of Insurance Commissioners launched its climate resilience disaster risk strategy for insurance based on state-specific data analytics[18]. The Global Shield reinforced its ability to bring modelling expertise to the doorstep of sovereigns[19]. The Resilient Planet Data Hub[20] showed how zooming into risk impact metrics can strengthen resilience. The entire list of initiatives is longer than would reasonably fit into these concluding words.

As we collaboratively work to close the protection gap, there is no such thing as "too advanced" or "generation 2" solutions. There are only accurate solutions, and we already live in the next generation area. The authors and contributors to this three-part publication hope to have demonstrated how the choice of underlying data influences the quality of risk financing solutions. As the list of technologies serving risk analytics grows, our experts are also providing risk views to specific propositions. At an industry event back in 2013, a senior representative of the Turkish earthquake risk pool shared his vision of flood as the 21st century's hazard. Ten years later, it looks like we have fully entered that vision, exacerbated by a myriad of other weather-related perils. The protection gap is widening as the risk universe continues to expand and to hinder the resilience of our societies. Digitalization has become a threat. But over these last ten years data quality has strongly improved, as African Risk Capacity CEO Lesley Ndlovu highlighted during the COP28 exchanges. And digitalization has also become a solution. On the growing threat of flooding, technological providers address very specific needs to observe the extent of floods using older and newer satellite technologies. Advanced modelling approaches enable us to integrate forecast and actual observation windows into flood footprints. The event map design presented earlier can be applied with such technologies. The combination of a complex risk data landscape and comprehensive modelling is bringing accurate, index-based risk solutions within the grasp of more people than ever before.

References

1. NOAA. (2002, August 21). After 10 years, hurricane Andrew gains strength. Retrieved from NOAA Press Release: https://www.nhc.noaa.gov/news/NOAA_pr_8-21-02.html
2. NOAA. (2017). National Weather Service. Retrieved from Hurricane Irma Local Report/Summary: https://www.weather.gov/mfl/hurricaneirma
3. Meteo France C.N.R.S de la Réunion. (2007). Météo La Flèche. Retrieved from Le cyclone Gamede à La Réunion: https://www.meteolafleche.com/Cyclone/2007/gamede.html
4. Hong Kong Observatory. (2019). Tropical Cyclones 2017. Hong-Kong.
5. US Geological Survey. (2023). Earthquake Hazards Program. Retrieved from ShakeMap: https://earthquake.usgs.gov/data/shakemap/
6. Artemis. (2019, June 21). Artemis. Retrieved from Peru cat bond pay out of USD60m for earthquake confirmed: https://www.artemis.bm/news/peru-cat-bond-pay-out-of-60m-for-earthquake-confirmed/
7. 7. OCHA Services >>> I don't find it- to be check with Stève
8. Global Human Settlement. (n.d.). Global Human Settlement Layer. Retrieved from GHS Population Grid: https://ghsl.jrc.ec.europa.eu/ghs_pop.php
9. Allend, T. I. (2008). An Atlas of ShakeMaps fro Selected Global Earthquakes. U.S. Geological Survey. Retrieved from extension://efaidnbmnnnibpcajpcglclefindmkaj/https://pubs.usgs.gov/of/2008/1236/downloads/OF08-1236_508.pdf
10. WMO. (2022, 12 14). Weather forecasting enters new era. Retrieved from wmo.int: https://public.wmo.int/en/media/news/weather-forecasting-enters-new-era

    WMO. (2023). Early Warning for All. Retrieved from public.wmo.int: https://public.wmo.int/en/earlywarningsforall

    WMO. (n.d.). Weather - Climate - Water. Retrieved from Global Observing System: https://public-old.wmo.int/en/programmes/global-observing-system
11. \WMO. (n.d.). WMO Extranet. Retrieved from Tropical Cyclone Regional Bodies: https://community.wmo.int/en/tropical-cyclone-regional-bodies
12. Willoughby, H. (2006). Parametric Representation of the Primary Hurricane Vortex. American Meteorological Society, 1102-1120.
13. NOAA. (2019, October 23). Office of Response and Restoration. Retrieved from Map of the Month: Hurricane Dorian: https://response.restoration.noaa.gov/map-month-hurricane-dorian
14. Harrouni, P. K. (2009). Building Construction Vulnerability and Inventory. Rabat: Faculté des Sciences, Université Mohammed V.
15. SCOR. (2021, 09 15). Launch of 'Heat Stress Protect' insurance to protect dairy income from climate change. Retrieved from scor.com: https://www.scor.com/en/news/launch-heat-stress-protect-insurance-protect-dairy-income-climate-change
16. Taj-Eddine Cherkaoui, A. E. (2012). Seismicity and Seismic Hazard in Morocco 1901-2010. Bulletin de l'Institut Scientifique(34), pp. 45-55.
17. Wikipedia. (2023). Modified Mercalli intensity scale. Retrieved from en.wikipedia.org: https://en.wikipedia.org/wiki/Modified_Mercalli_intensity_scale
18. National Association of Insurance Commissioners. (2023, 12 01). National Climate Resilience Strategy for Insurance. Retrieved from content.naic.org: https://content.naic.org/sites/default/files/draft-naic-national-climate-resilience-strategy-12-1-2023-updated.pdf
19. Global Shield. (2023, 12 02). Global Shield gains more momentum at COP28. Retrieved from Global Shield against Climate Risks: https://www.globalshield.org/news/global-shield-gains-more-momentum-at-cop28
20. Resilient Planet Data Hub. (2023, 12 14). Resilient Planet Data Hub announced at COP28. Retrieved from Resilient Planet Data Hub: https://resilient-planet-data.org/latest/Resilient-Planet-Data-Hub-announced-at-COP28

This article was written by:

Stève UDRIOT
Senior Underwriter Alternative Solutions &
Head of Public Authorities
sudriot@scor.com

Co-authors:

Ismael RIEDEL
Senior Cat Analyst
iriedel@scor.com

Liu YE
Catastrophe Risk Manager
lye@scor.com

Contributor:

Henry BOVY
Accumalation Team Property Lead
hbovy@scor.com

Please feel free to visit us at scor.com

SCOR SE
5 avenue Kléber - 75795 PARIS Cedex 16
France
scorglobalpc@scor.com

SCOR
The Art & Science of Risk

April 2024